Asymptotic analysis of drug dissolution in two layers having widely differing diffusivities

MICHAEL VYNNYCKY[†,*]

Division of Processes, Department of Materials Science and Technology, KTH Royal Institute of Technology, Brinellvägen 23, 100 44 Stockholm, Sweden.
[†]Corresponding author: michaelv@kth.se

SEAN MCKEE

Department of Mathematics and Statistics, University of Strathclyde, Livingstone Tower, 26 Richmond Street, Glasgow, G1 1XH, UK

MARTIN MEERE

Department of Applied Mathematics, NUI Galway, Galway, Ireland.

CHRIS MCCORMICK

Department of Biomedical Engineering, University of Strathclyde, Glasgow, G4 0NW, UK

AND

SEAN MCGINTY

Division of Biomedical Engineeering, University of Glasgow, Glasgow, G1 1XH, UK

This paper is concerned with a diffusion-controlled moving-boundary problem in drug dissolution, in which the moving front passes from one medium to another for which the diffusivity is many orders of magnitude smaller. The classical Neumann similarity solution holds while the front is passing through the first layer, but this breaks down in the second layer. Asymptotic methods are used to understand what is happening in the second layer. Although this necessitates numerical computation, one interesting outcome is that only one calculation is required, no matter what the diffusivity is for the second layer.

1. Introduction

Moving boundary problems arise in many industrial, environmental and technological applications. These include the freezing and defrosting of food (Bakal et al. (1970)), swelling grains or polymers (Anderson (1982)), etching (Vuik & Cuvelier (1985)), dendritic solidification (Schmidt (1996)), metal processing (Segal et al. (1998)), crystal growth (Conti (2001); Libbrecht (2005)), chemically-reactive and heat-diffusive liquids surrounded by ice (Fila & Souplet (2001)), laser-induced heating and melting in solids (Shen et al. (2001)), environmental engineering and thermal energy storage systems (Mehling & Cabeza (2002); Zalba et al. (2003)), shore-line movement with ocean depth (Lorenzo-Trueba & Voller

[*]Present address: Department of Applied Mathematics and Statistics, Institute of Mathematical and Computer Sciences, University of São Paulo at São Carlos, PO Box 668, 13560-970 São Carlos, São Paulo, Brazil

(2010)), supercooling/superheating phenomena (Gotz & Zaltzman (1995); Tabakova et al. (2010)), solidification of nanostructure-enhanced phase change materials (El-Hasadi & Khodadadi (2013)), porous thermal heart processes (Trelles & Dufly (2003)), phenomena involving nano-sized particles (McCue et al. (2009); Fan et al. (2015)) and melting and solidification enhancement (Sharifi et al. (2014)).

Although moving boundary problems date back to Stefan's original paper (Stefan (1890)), the area received a reawakening with a meeting held in Oxford in 1974 (Ockendon & Hodgkins (1975)). Two papers stand out in the proceedings. Tayler (1975) considers a mathematical formulation of the Stefan problem and its generalizations: in particular, he discusses problems that do not have a continuous second derivative and develops a weak formulation which allows for the so-called mushy region. Ockendon (1975), on the other hand, discusses an integral formulation, the use of transform techniques and asymptotic methods.

When a problem is well-characterized by a one-dimensional system of equations, analytic solutions are often readily obtained. For example, if the system comprises a one-dimensional diffusion equation with appropriate initial and boundary conditions, as well as a Stefan condition to track the position of the moving boundary, then it can often be shown that the problem is self-similar, and through a similarity reduction one may convert the original partial differential equation to an ordinary differential equation (ODE). Some discussion of the analytic solutions of moving boundary problems arising in diffusive systems, such as the Neumann solution to the classical Stefan problem, can also be found in Crank (1984).

When this is not possible, many authors resort to numerical methods. An early review of four different numerical techniques, including immobilization of the free surface through an appropriate coordinate transformation and the enthalpy method, was carried out by Furzeland (1980). Indeed, most of the authors cited above have employed a variety of numerical methods. Text books dealing with these techniques include Crank (1984), Hill (1987), Gupta (2003) and Tarzia (2011).

A particular class of one-dimensional Stefan problem for which one would expect numerical methods to be necessary is when the diffusivity is not constant, although there are some notable analytic exceptions even to this for particular non-linear forms for the diffusivity (Cho & Sunderland (1974); Hill & Hart (1986); Rogers (1986); Natale & Tarzia (2003); Briozzo et al. (2007); Voller & Falcini (2013)). On the other hand, the moving boundary value problem in this paper has a diffusivity which is spatially dependent in the sense that it takes one constant value in one part of the domain and another constant value in the other part; in addition, the two constants differ by several orders of magnitude. This is the situation that arose in a recent experimental and theoretical investigation Vo et al. (2018) concerning drug release from polymer-free coronary stents with microporous surfaces. The theoretical analysis led to the following one-dimensional, one-phase, diffusion-controlled moving boundary problem:

$$\frac{\partial c}{\partial t} = \frac{\partial}{\partial x}\left(D(x)\frac{\partial c}{\partial x}\right), \qquad x > s(t), t > 0, \tag{1.1}$$

$$c = c_s, \quad -D(x)\frac{\partial c}{\partial x} = \frac{\mathrm{d}s}{\mathrm{d}t}(c_s - c_0) \quad \text{at } x = s(t), t > 0, \tag{1.2}$$

$$c \to 0 \quad \text{as } x \to \infty, t > 0, \tag{1.3}$$

$$s(0) = L_d, \quad c(x,0) = 0 \quad \text{for } x > L_d. \tag{1.4}$$

Here, c represents the concentration of the drug, $s(t)$ a free surface between the dissolved and undissolved drug, L_d denotes the thickness of the drug layer initially, which occupies the region $0 < x < L_d$,
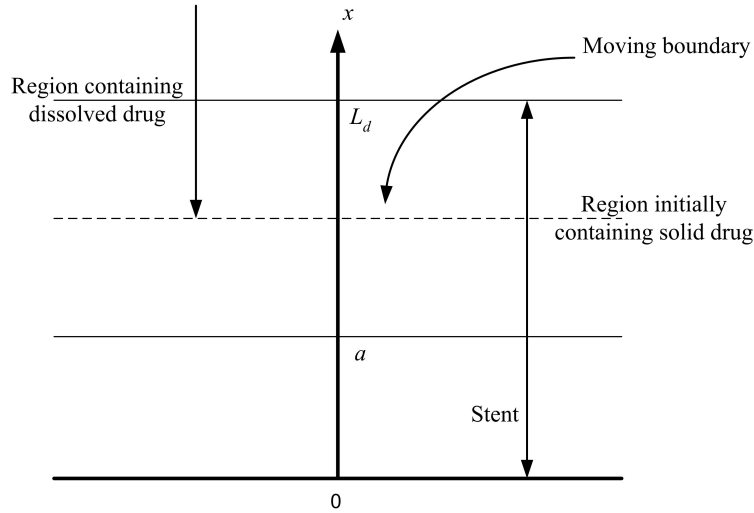
FIG. 1. Schematic showing the problem considered by Vo et al. (2018). The region $0 < x < L_d$ initially contains drug at uniform concentration c_0. For $t > 0$, drug dissolves on a moving front (where the concentration is identically c_s, the solubility of the drug), starting at $x = L_d$. Drug dissolution is complete when the moving boundary tracks back to $x = 0$. Dissolved drug diffuses out of the system into a release medium which is considered to be infinite. The diffusivity of the dissolved drug in the region $0 < x < a$ is much smaller than that in the region $x > a$.

$a < L_d$ denotes the mean position of the microporous region (also containing drug), c_s the solubility of the drug and c_0 the initial constant concentration for $x < L_d$. The spatially dependent diffusivity is

$$D(x) = \begin{cases} D_e \, (< D_w) & \text{if } 0 < x \leqslant a_- \\ D_w & \text{if } x \geqslant a_+ \end{cases} . \tag{1.5}$$

We note that the resulting model may bear a passing similarity to moving boundary problems for swelling-controlled drug release (Cohen & Erneux (1988a,b)), although the mechanism is not the same and neither is our handling of the analysis.

The problem given by (1.1)-(1.5) gives rise to a two-stage release of drug, which is explained with the help of Figure 1. In Stage 1, the drug dissolves on a moving front in the region $a < x < L_d$ and diffuses out of the system. In Stage 2, the moving boundary has tracked back to $x = a$ and the drug then proceeds to dissolve from the rough surface region where it is released at a slower rate. For Stage 1 $(s(t) > a)$, McGinty et al. (2015) and Vo et al. (2018) found that the classical Neumann solution holds, namely

$$s(t) = L_d - \theta \sqrt{t}, \quad c(x,t) = \frac{c_s \mathrm{erfc}\left(\frac{x - L_d}{2\sqrt{D_w t}} \right)}{\mathrm{erfc}\left(-\frac{\theta}{2\sqrt{D_w}} \right)}, \quad L_d - \theta\sqrt{t} < x < \infty, \ \ 0 < t < t_a, \tag{1.6}$$

where θ is determined by

$$\frac{\theta}{2\sqrt{D_w}} \exp\left(\frac{\theta^2}{4D_w} \right) \mathrm{erfc}\left(-\frac{\theta}{2\sqrt{D_w}} \right) = \frac{1}{\sqrt{\pi}} \frac{c_s}{c_0 - c_s}. \tag{1.7}$$

Note that (1.7) will have a positive solution for θ, which is required by (1.6) provided that $c_0 > c_s$; moreover, the solution will be unique because the left-hand side is an increasing function for $\theta > 0$. As for (1.6) itself, it is valid until $t = t_a$, whereupon $s(t_a) = a$, so that

$$t_a = \frac{(L_d - a)^2}{\theta^2}. \tag{1.8}$$

Note that the transcendental equation (1.7) is the same as that obtained by Paul & McSpadden (1976) in a problem for the diffusional release of a solute from a polymer matrix. Observe also that if $c_s > c_0$, we obtain $\theta < 0$ and the solution is identical to that of the freezing of a supercooled liquid, originally considered by Carslaw & Jaeger (1959) and referred to more recently by Voller (2006); thus, although not commented on by McGinty et al. (2015) or Vo et al. (2018), it appears that (1.6) with $c_s < c_0$ is a solution that does not have an exact counterpart in the literature. Furthermore, at $t = t_a$,

$$c(x, t_a) = c_a(x) = \frac{c_s \operatorname{erfc}\left(\frac{x - L_d}{2\sqrt{D_w t_a}}\right)}{\operatorname{erfc}\left(-\frac{\theta}{2\sqrt{D_w}}\right)}, \quad a \leqslant x < \infty. \tag{1.9}$$

For Stage 2, a numerical procedure was employed.

However, the fact that $D_e \ll D_w$ suggests that formal asymptotics may be a useful tool in this context. Indeed, such methods have been used for Stefan-like problems before, although not for problems exactly like this one. Comparatively recent examples are the papers by Struckmeier & Unterreiter (2001), Evans & King (2000), King & Evans (2005) and McCue et al. (2008), although in each case the diffusivities on either side of the moving boundary differ by orders of magnitude; here, on the other hand, the front passes from a highly diffusive medium to one that is not.

In this paper, we will be concerned with the release of drug from the system during Stage 2. In particular, we adopt an asymptotic approach to derive approximate solutions for this phase of release. In Section 2, we start by presenting the equations that represent Stage 2 of the release. We then outline our asymptotic argument. In Section 3, we provide results including comparisons with the numerical solutions obtained by Vo et al. (2018), whilst the findings are discussed in Section 4.

2. Stage 2 $(s(t) < a)$

The Stage 2 problem, when $t > t_a$, may then be formulated in dimensional form as:

$$\frac{\partial c}{\partial t} = \frac{\partial}{\partial x}\left(D_w \frac{\partial c}{\partial x}\right), \qquad a < x < \infty, \quad t > t_a, \tag{2.1}$$

$$\frac{\partial c}{\partial t} = \frac{\partial}{\partial x}\left(D_e \frac{\partial c}{\partial x}\right), \qquad s(t) < x < a, \quad t > t_a, \tag{2.2}$$

$$c = c_s, \quad -D_e \frac{\partial c}{\partial x} = \frac{\mathrm{d}s}{\mathrm{d}t}(c_s - c_0), \quad \text{at } x = s(t), \tag{2.3}$$

$$c \to 0, \quad \text{as } x \to \infty, \tag{2.4}$$

$$s(t_a) = a, \quad c(x, t_a) = c_a(x), \quad x \geqslant a. \tag{2.5}$$

Parameter	Value
a	1×10^{-6}-4×10^{-6} m
c_0/c_s	10-200
D_e	2.5×10^{-17}-5×10^{-16} m^{2}s^{-1}
D_w	5×10^{-11} m^{2}s^{-1}
L_d	10^{-5} m

Table 1. Model parameters

In addition, we require

$$[c]_-^+ = 0 \quad \text{at } x = a, \tag{2.6}$$

$$\left(D_e \frac{\partial c}{\partial x}\right)_- = \left(D_w \frac{\partial c}{\partial x}\right)_+ \quad \text{at } x = a. \tag{2.7}$$

We non-dimensionalize the problem by setting

$$X = \frac{x}{a}, \quad T = \frac{t - t_a}{a^2/D_e}, \quad S = \frac{s}{a}, \quad C = \frac{c}{c_s}, \quad C_a = \frac{c_a}{c_s}, \tag{2.8}$$

with typical values for the dimensional parameters, as considered by Vo et al. (2018), being given in Table 1. This gives

$$\delta \frac{\partial C}{\partial T} = \frac{\partial^2 C}{\partial X^2}, \qquad 1 < X < \infty, \quad T > 0, \tag{2.9}$$

$$\frac{\partial C}{\partial T} = \frac{\partial^2 C}{\partial X^2}, \qquad S(T) < X < 1, \quad T > 0, \tag{2.10}$$

$$C = 1, \quad -\frac{\partial C}{\partial X} = \frac{\mathrm{d}S}{\mathrm{d}T}\left(1 - \frac{c_0}{c_s}\right), \quad \text{at } X = S(T), \tag{2.11}$$

$$C \to 0, \quad \text{as } X \to \infty, \tag{2.12}$$

$$S(0) = 1, \quad C(X, 0) = C_a(X), \quad X \geqslant 1, \tag{2.13}$$

where $\delta = D_e/D_w \ll 1$ and

$$C_a(X) = \frac{\text{erfc}\left(\frac{aX - L_d}{2\sqrt{D_w t_a}}\right)}{\text{erfc}\left(-\frac{\theta}{2\sqrt{D_w}}\right)}. \tag{2.14}$$

In addition, we have

$$[C]_-^+ = 0 \quad \text{at } X = 1, \tag{2.15}$$

$$\delta\left(\frac{\partial C}{\partial X}\right)_- = \left(\frac{\partial C}{\partial X}\right)_+ \quad \text{at } X = 1. \tag{2.16}$$

Considering (2.9)-(2.16) at leading order in δ, we have just

$$\frac{\partial^2 C}{\partial X^2} \approx 0, \quad 1 < X < \infty, \tag{2.17}$$

$$C \to 0, \quad \text{as } X \to \infty, \tag{2.18}$$

$$\left(\frac{\partial C}{\partial X}\right)_+ \approx 0 \quad \text{at } X = 1, \tag{2.19}$$

which would require $C \equiv 0$, for $X > 1$. For $X < 1$, we would have

$$\frac{\partial C}{\partial T} = \frac{\partial^2 C}{\partial X^2}, \qquad S(T) < X < 1, \quad T > 0, \tag{2.20}$$

$$C = 1, \quad -\frac{\partial C}{\partial X} = \frac{\mathrm{d}S}{\mathrm{d}T}\left(1 - \frac{c_0}{c_s}\right), \quad \text{at } X = S(T). \tag{2.21}$$

Also, (2.15) would imply

$$C = 0 \text{ at } X = 1.$$

In fact, this cannot hold for all time, since $C = 1$ at $X = 1$ at $T = 0$, i.e. in dimensional form, $c = c_s$ when $x = s(t_a) = a$.

2.1 *Asymptotic argument*

The above suggests that we must try to retain the term on the left-hand side of (2.9), which can be achieved if $T \sim \delta$. This will mean that the left-hand side of (2.10) will be large, and would need to be balanced by the right-hand side, indicating that $1 - X$, i.e. the width of the lower region, must be of an appropriately small width. If we suppose that $1 - X \sim [X]$, where $[X] \ll 1$ and is still to be determined, then there are only two possibilities: $[X] \sim \delta$, so that the full form of (2.16) is retained and $[X] \sim \delta^{1/2}$. However, the first of these does not lead to a distinguished limit, but merely results in an inconsistency in the leading-order equations for C and leaves S undetermined; thus, we choose the second option. Setting

$$1 - X = \delta^{1/2}\tilde{X}, \quad 1 - S = \delta^{1/2}\tilde{S}, \quad T = \delta\tilde{T}, \tag{2.22}$$

we also introduce regular perturbation expansions for C and $\tilde{S}$ of the form

$$C = C^{(0)} + \delta^{1/2}C^{(1)} + O(\delta), \tag{2.23}$$

$$\tilde{S} = \tilde{S}^{(0)} + \delta^{1/2}\tilde{S}^{(1)} + O(\delta), \tag{2.24}$$

and consider the leading-order problem at $O(1)$; the expansions given above are uniformly valid, and there will be no need to consider higher-order problems. Dropping the superscript $^{(0)}$, we have

$$\frac{\partial C}{\partial \tilde{T}} = \frac{\partial^2 C}{\partial X^2}, \qquad 1 < X < \infty, \quad \tilde{T} > 0, \tag{2.25}$$

subject to

$$C \to 0, \quad \text{as } X \to \infty, \tag{2.26}$$

and, from (2.16),

$$\frac{\partial C}{\partial X} = 0 \quad \text{at } X = 1. \tag{2.27}$$

Also, (2.10) becomes

$$\frac{\partial C}{\partial \tilde{T}} = \frac{\partial^2 C}{\partial \tilde{X}^2}, \qquad \tilde{X} > 0, \quad \tilde{T} > 0, \tag{2.28}$$

subject to

$$C = C_+ \left(\tilde{T} \right) \quad \text{at } \tilde{X} = 0, \tag{2.29}$$

$$C = 1, \quad -\frac{\partial C}{\partial \tilde{X}} = \frac{\mathrm{d}\tilde{S}}{\mathrm{d}\tilde{T}}(1 - \frac{c_0}{c_s}), \quad \text{at } \tilde{X} = \tilde{S}\left(\tilde{T}\right), \tag{2.30}$$

where

$$C_+ \left(\tilde{T} \right) = C \left(X = 1_+, \tilde{T} \right). \tag{2.31}$$

Note that $C_+ (0) = 1$, i.e. $c(a, t_a) = c_s$.

We observe that the problem for $X > 1$ (i.e. $x > a$) decouples from that for $X < 1$ ($x < a$); we now solve these in turn.

2.2 $X \geqslant 1$

First, we solve the problem for $X \geqslant 1, \tilde{T} \geqslant 0$, corresponding to $x \geqslant a, t \geqslant t_a$. From Section 2.1, the problem at hand is, on setting $\xi = X - 1$,

$$\frac{\partial C}{\partial \tilde{T}} = \frac{\partial^2 C}{\partial \xi^2}, \tag{2.32}$$

subject to

$$\frac{\partial C}{\partial \xi} = 0 \quad \text{at } \xi = 0, \tag{2.33}$$

$$C \to 0 \quad \text{as } \xi \to \infty, \tag{2.34}$$

$$C = C_a \left(\xi \right) \quad \text{at } \tilde{T} = 0, \tag{2.35}$$

where

$$C_a \left(\xi \right) = \frac{\operatorname{erfc}\left(\frac{a(1+\xi) - L_d}{2\sqrt{D_w t_a}} \right)}{\operatorname{erfc}\left(-\frac{\theta}{2\sqrt{D_w}} \right)}. \tag{2.36}$$

Using Fourier transforms, we obtain

$$C\left(\xi, \tilde{T}\right) = \frac{1}{2\sqrt{\pi \tilde{T}}} \int_0^\infty C_a \left(\xi' \right) \left\{ \exp\left(-\frac{(\xi - \xi')^2}{4\tilde{T}} \right) + \exp\left(-\frac{(\xi + \xi')^2}{4\tilde{T}} \right) \right\} \mathrm{d}\xi'. \tag{2.37}$$

Before we can tackle the second problem (i.e. the case $X < 1$), we shall require $C_+ \left(\tilde{T} \right) = C \left(\xi = 0, \tilde{T} \right)$ for condition (2.29), i.e.

$$C_+ \left(\tilde{T} \right) = \frac{1}{\sqrt{\pi \tilde{T}}} \int_0^\infty C_a \left(\xi' \right) \exp\left(-\frac{\xi'^2}{4\tilde{T}} \right) \mathrm{d}\xi'. \tag{2.38}$$

Putting $z = \xi'/2\sqrt{\tilde{T}}$, we have

$$C_+(\tilde{T}) = \frac{2}{\sqrt{\pi}} \int_0^\infty C_a\left(2z\sqrt{\tilde{T}}\right) e^{-z^2} \, \mathrm{d}z$$

$$= C_a(0) + \frac{2\sqrt{\tilde{T}}}{\sqrt{\pi}} \frac{\mathrm{d}C_a}{\mathrm{d}\xi}(0) + O(\tilde{T}), \qquad (2.39)$$

where we have used a Taylor series expansion for C_a about $z = 0$. Now, on using (2.36) and recalling equation (1.8), we note that $C_a(0) = 1$ and that

$$\frac{\mathrm{d}C_a}{\mathrm{d}\xi}(0) = -\frac{a}{\sqrt{\pi D_w t_a}} \frac{\exp\left(-\frac{(a-L_d)^2}{4D_w t_a}\right)}{\mathrm{erfc}\left(-\frac{\theta}{2\sqrt{D_w}}\right)}.$$

So, we have, for small $\tilde{T}$,

$$C_+(\tilde{T}) = 1 - \left\{ \frac{2a}{\pi\sqrt{D_w t_a}} \frac{\exp\left(-\frac{(a-L_d)^2}{4D_w t_a}\right)}{\mathrm{erfc}\left(-\frac{\theta}{2\sqrt{D_w}}\right)} \right\} \sqrt{\tilde{T}} + O(\tilde{T}). \qquad (2.40)$$

However, to determine $C(0, \tilde{T})$ for all $\tilde{T}$, we need to revert to (2.38) with $z = \xi'/2\sqrt{\tilde{T}}$, which gives

$$C_+(\tilde{T}) = \frac{2}{\sqrt{\pi}\mathrm{erfc}\left(-\frac{\theta}{2\sqrt{D_w}}\right)} \int_0^\infty \mathrm{erfc}\left(f(z,\tilde{T})\right) e^{-z^2} \, \mathrm{d}z, \qquad (2.41)$$

where

$$f(z,\tilde{T}) = \frac{a\left(1 + 2z\sqrt{\tilde{T}}\right) - L_d}{2\sqrt{D_w t_a}}.$$

Differentiating with respect to $\tilde{T}$, we have

$$\frac{\mathrm{d}C_+}{\mathrm{d}\tilde{T}} = -\frac{2a}{\pi\mathrm{erfc}\left(-\frac{\theta}{2\sqrt{D_w}}\right)\sqrt{D_w t_a \tilde{T}}} \int_0^\infty z e^{-\left(z^2 + f^2(z,\tilde{T})\right)} \, \mathrm{d}z. \qquad (2.42)$$

Rearranging the argument in the exponential in (2.42), we have

$$z^2 + \frac{\left(2az\sqrt{\tilde{T}} + a - L_d\right)^2}{4D_w t_a} = \mathscr{A}(\tilde{T})\left\{\left(z + \mathscr{B}(\tilde{T})\right)^2 + \mathscr{C}(\tilde{T})\right\},$$

where

$$\mathscr{A}(\tilde{T}) = 1 + \frac{a^2\tilde{T}}{D_w t_a}, \qquad (2.43)$$

$$\mathscr{B}(\tilde{T}) = \frac{\left[\frac{(a-L_d)a\sqrt{\tilde{T}}}{D_w t_a}\right]}{2\left(1 + \frac{a^2\tilde{T}}{D_w t_a}\right)}, \qquad (2.44)$$

$$\mathscr{C}(\tilde{T}) = \frac{\frac{(a-L_d)^2}{4D_w t_a}}{\left(1 + \frac{a^2\tilde{T}}{D_w t_a}\right)} - \frac{\left[\frac{(a-L_d)a\sqrt{\tilde{T}}}{D_w t_a}\right]^2}{4\left(1 + \frac{a^2\tilde{T}}{D_w t_a}\right)^2}; \qquad (2.45)$$

it is now possible to write the integral in (2.42) in the form

$$\int_0^\infty z e^{-\left\{\mathscr{A}(\tilde{T})\left[(z+\mathscr{B}(\tilde{T}))^2+\mathscr{C}(\tilde{T})\right]\right\}}\,\mathrm{d}z. \tag{2.46}$$

Next, with $\zeta = z + \mathscr{B}(\tilde{T})$ and later $\xi = \mathscr{A}^{1/2}(\tilde{T})\,\zeta$, we have

$$\int_0^\infty z e^{-\mathscr{A}(\tilde{T})\left[(z+\mathscr{B}(\tilde{T}))^2+\mathscr{C}(\tilde{T})\right]}\,\mathrm{d}z$$
$$= \frac{1}{2}e^{-\mathscr{A}(\tilde{T})\mathscr{C}(\tilde{T})}\left\{\frac{e^{-\mathscr{A}(\tilde{T})\mathscr{B}^2(\tilde{T})}}{\mathscr{A}(\tilde{T})} - \frac{\pi^{1/2}\mathscr{B}(\tilde{T})}{\mathscr{A}^{1/2}(\tilde{T})}\mathrm{erfc}\left(\mathscr{A}^{1/2}(\tilde{T})\,\mathscr{B}(\tilde{T})\right)\right\}. \tag{2.47}$$

Hence, we have the following first-order ODE for $C_+(\tilde{T})$:

$$\frac{\mathrm{d}C_+}{\mathrm{d}\tilde{T}} = -\frac{a e^{-\mathscr{A}(\tilde{T})\mathscr{C}(\tilde{T})}}{\pi\,\mathrm{erfc}\left(-\frac{\theta}{2\sqrt{D_w}}\right)\sqrt{D_w t_a}\sqrt{\tilde{T}}}\left\{\frac{e^{-\mathscr{A}(\tilde{T})\mathscr{B}^2(\tilde{T})}}{\mathscr{A}(\tilde{T})} - \frac{\pi^{1/2}\mathscr{B}(\tilde{T})}{\mathscr{A}^{1/2}(\tilde{T})}\mathrm{erfc}\left(\mathscr{A}^{1/2}(\tilde{T})\,\mathscr{B}(\tilde{T})\right)\right\}, \tag{2.48}$$

subject to

$$C_+ = 1 \quad \text{at } \tilde{T} = 0. \tag{2.49}$$

Checking $\mathscr{A}(\tilde{T}), \mathscr{B}(\tilde{T}), \mathscr{C}(\tilde{T})$ in the limit as $\tilde{T} \to 0$, we have

$$\mathscr{A}(0) = 1, \quad \mathscr{B}(0) = 0, \quad \mathscr{C}(0) = \frac{(a-L_d)^2}{4D_w t_a}, \tag{2.50}$$

so that

$$\frac{\mathrm{d}C_+}{\mathrm{d}\tilde{T}} \sim \left(-\frac{a e^{-(a-L_d)^2/4D_w t_a}}{\pi\,\mathrm{erfc}\left(-\frac{\theta}{2\sqrt{D_w}}\right)\sqrt{D_w t_a}}\right)\frac{1}{\sqrt{\tilde{T}}}. \tag{2.51}$$

2.3 $X < 1$

For this region, we require to solve (2.28)-(2.31). Note that, from the solution for $X > 1$, we have already found in (2.40) that, for small $\tilde{T}$,

$$C_+(\tilde{T}) - 1 \sim \tilde{T}^{1/2}. \tag{2.52}$$

Moreover, at $\tilde{T} = 0$, the region that we are solving in, i.e. $0 < \tilde{X} < \tilde{S}(\tilde{T})$, has zero width, which suggests that it may be appropriate to proceed in terms of similarity or similarity-like variables. For this purpose, we set

$$C - 1 = \tilde{T}^{1/2}F(\eta, \tilde{T}), \qquad \eta = \frac{\tilde{X}}{\tilde{S}(\tilde{T})}, \tag{2.53}$$

so that equation (2.28) becomes

$$\frac{\tilde{S}^2(\tilde{T})F}{2\tilde{T}} + \left(\tilde{S}^2(\tilde{T})\frac{\partial F}{\partial \tilde{T}} - \tilde{S}(\tilde{T})\frac{\mathrm{d}\tilde{S}}{\mathrm{d}\tilde{T}}\eta\frac{\partial F}{\partial \eta}\right) = \frac{\partial^2 F}{\partial \eta^2}, \tag{2.54}$$

subject to

$$1 + \tilde{T}^{1/2}F = C_+\left(\tilde{T}\right) \quad \text{at } \eta = 0, \tag{2.55}$$

$$F = 0 \quad \text{at } \eta = 1, \tag{2.56}$$

$$-\frac{\partial F}{\partial \eta} = \frac{\tilde{S}\left(\tilde{T}\right)}{\tilde{T}^{1/2}}\frac{d\tilde{S}}{d\tilde{T}}(1 - \frac{c_0}{c_s}) \quad \text{at } \eta = 1. \tag{2.57}$$

It is now required that (2.54)-(2.57) behave in a self-consistent manner as $\tilde{T} \to 0$; by this, we mean that we should obtain an ODE, subject to the requisite number of boundary conditions. This can be done by taking

$$\frac{\tilde{S}\left(\tilde{T}\right)}{\tilde{T}^{1/2}}\frac{d\tilde{S}}{d\tilde{T}} \sim 1, \tag{2.58}$$

as suggested by (2.57). We obtain $\tilde{S}\left(\tilde{T}\right) \sim \tilde{T}^{3/4}$, which ensures a sensible leading-order balance in (2.54) and (2.57). Setting $\tilde{S}\left(\tilde{T}\right) = \lambda\tilde{T}^{3/4} + ..$, where λ is a positive constant to be determined, equation (2.54) becomes, in the limit as $\tilde{T} \to 0$,

$$\frac{d^2 F_0}{d\eta^2} = 0, \tag{2.59}$$

where

$$F_0\left(\eta\right) := \lim_{\tilde{T}\to 0} F\left(\eta, \tilde{T}\right). \tag{2.60}$$

subject to

$$F_0 = \mu \quad \text{at } \eta = 0, \tag{2.61}$$

$$F_0 = 0 \quad \text{at } \eta = 1, \tag{2.62}$$

$$-\frac{dF_0}{d\eta} = \frac{3}{4}\lambda^2(1 - \frac{c_0}{c_s}) \quad \text{at } \eta = 1, \tag{2.63}$$

where μ is a constant given by

$$\mu = \lim_{\tilde{T}\to 0} \frac{(C)_{X=1} - 1}{\tilde{T}^{1/2}}. \tag{2.64}$$

Note that μ can be determined, and we will do so shortly, from the solution for $X > 1$. Thus, solving (2.59) subject to (2.61)-(2.63) gives

$$F_0\left(\eta\right) = \mu\left(1 - \eta\right), \tag{2.65}$$

with

$$\mu = \frac{3}{4}\lambda^2(1 - \frac{c_0}{c_s}), \tag{2.66}$$

i.e.

$$\lambda = \pm\left(\frac{4\mu}{3(1 - c_0/c_s)}\right)^{1/2}. \tag{2.67}$$

Clearly, we need to take the positive sign to ensure that $\tilde{S}$ increases, i.e. S decreases. Also, since $c_0 > c_s$, it is clear that we will need $\mu < 0$; we return to this point shortly.

Note also that it is possible to determine μ without solving (2.32)-(2.35). Near $X = 1$, we have

$$C_a = 1 + (X - 1)\left(\frac{dC_a}{dX}\right)_{X=1} + ... \tag{2.68}$$

where, on using (2.14),

$$\alpha := \left(\frac{\mathrm{d}C_a}{\mathrm{d}X}\right)_{X=1} = -\frac{a\exp\left(-\frac{(L_d-a)^2}{4D_w t_a}\right)}{\sqrt{\pi D_w t_a}\,\mathrm{erfc}\left(-\frac{\theta}{2\sqrt{D_w}}\right)}. \tag{2.69}$$

We consider the small and positive $X - 1$ and small $\tilde{T}$ behaviour of (2.32)-(2.35) by setting $\xi = X - 1$, as in section 2.2, and

$$C = 1 + \tilde{T}^{1/2}G\left(\zeta,\tilde{T}\right), \quad \zeta = \xi/\tilde{T}^{1/2}. \tag{2.70}$$

Equation (2.32) becomes

$$\tilde{T}\frac{\partial G}{\partial \tilde{T}} + \frac{G}{2} - \frac{\zeta}{2}\frac{\partial G}{\partial \zeta} = \frac{\partial^2 G}{\partial \zeta^2}. \tag{2.71}$$

Now, in the limit as $\tilde{T} \to 0$, (2.71) becomes

$$\frac{G_0}{2} - \frac{\zeta}{2}\frac{\mathrm{d}G_0}{\mathrm{d}\zeta} = \frac{\mathrm{d}^2 G_0}{\mathrm{d}\zeta^2}, \tag{2.72}$$

where

$$G_0\left(\zeta\right) := \lim_{\tilde{T}\to 0} G\left(\zeta,\tilde{T}\right). \tag{2.73}$$

Equation (2.72) has the general solution

$$G_0 = K_1\zeta + K_2\left(\pi\zeta\,\mathrm{erf}\left(\frac{\zeta}{2}\right) + 2\sqrt{\pi}\exp\left(-\frac{\zeta^2}{4}\right)\right), \tag{2.74}$$

where K_1 and K_2 are constants to be determined. Clearly, (2.72) must have two boundary conditions. One of these comes from (2.33), and is

$$\frac{\mathrm{d}G_0}{\mathrm{d}\zeta} = 0 \quad \text{at } \zeta = 0. \tag{2.75}$$

The other comes from matching G_0 as $\zeta \to \infty$ to C_a and is

$$\frac{\mathrm{d}G_0}{\mathrm{d}\zeta} \to \alpha \quad \text{as } \zeta \to \infty. \tag{2.76}$$

Since

$$\frac{\mathrm{d}G_0}{\mathrm{d}\zeta} = K_1 + K_2\pi\,\mathrm{erf}\left(\frac{\zeta}{2}\right), \tag{2.77}$$

we quickly see that

$$K_1 = 0, \quad K_2 = \frac{\alpha}{\pi}, \tag{2.78}$$

whence

$$G_0 = \alpha\left(\zeta\,\mathrm{erf}\left(\frac{\zeta}{2}\right) + \frac{2}{\sqrt{\pi}}\exp\left(-\frac{\zeta^2}{4}\right)\right); \tag{2.79}$$

ultimately, this leads to

$$\mu = G_0\left(0\right) = \frac{2\alpha}{\pi^{1/2}}. \tag{2.80}$$

Finally, recall from the discussion after equation (2.67) that we needed $\mu < 0$. Now, equation (2.80) implies that we will need $\alpha < 0$; from equation (2.69), we see that this will clearly be the case.
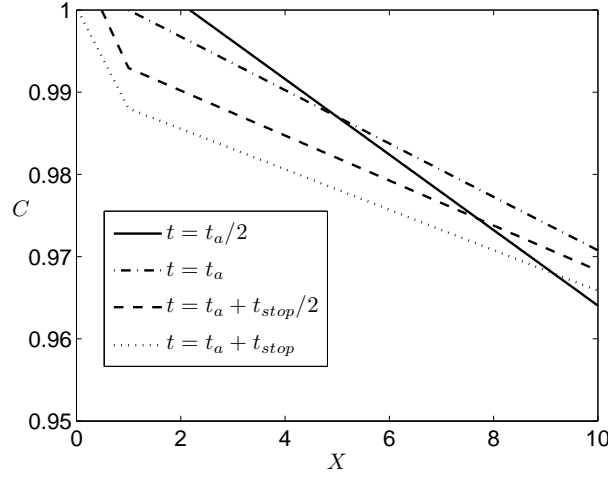
FIG. 2. C vs. X for four different values of t for $\delta = 0.2$, as obtained by solving (A.3) and (A.4), subject to (A.5)-(A.8) and (A.12). t_a and t_{stop} are approximately 2350 and 3760 seconds, respectively.

3. Results

The main numerical task is to solve equation (2.54), subject to (2.55)-(2.57); this constitutes a moving boundary problem for F and $\tilde{S}$. However, (2.55) contains $C_+\left(\tilde{T}\right)$, which must itself be solved for numerically via the first-order ODE (2.48), subject to (2.49). To illustrate our ideas, we will vary the value of D_e, so as to see the effect of δ, using the parameters given in Table 1; in particular, we take $a = 0.2L_d$ and $c_0/c_s = 50$ throughout.

However, before presenting results for which δ is very small, we will first consider the behaviour of the solution when δ is not so small; we take $\delta = 0.2$. For such a high value of δ, we would not expect the asymptotic analysis developed above to be valid. For this reason, further analysis was developed in order to be able to solve the full original governing equations, (2.9)-(2.16), numerically. This is given in Appendix A, as are details of the numerical method used to solve the equations; we note in passing that we use a similar method to solve the asymptotically reduced equations (2.54)-(2.57) also. Fig. 2 shows C as a function of X for four different values of $\tilde{T}$. These correspond to $t = t_a/2, t_a, t_a + t_{stop}/2, t_a + t_{stop}$, where t_{stop} is the time taken for the front to move from $X = 1$ to $X = 0$, i.e. $x = a$ to $x = 0$; thus, the first two curves are simply the similarity solution from (1.6), whereas the second two are numerical solutions. Evident in Fig. 2 is the discontinuity in the slope of C, once the moving boundary enters the second layer, i.e. at $X = 1$. Observe also that, even though the plot extends as far as $X = 10$, the value of C is far short of its far-field value for all four curves; this is accounted for in Appendix A also.

Next, we note that we are ultimately interested in determining the time at which the front reaches $x = 0$; this corresponds to the time at which $\tilde{S} = 1/\delta^{1/2}$. Whilst this will, of course, depend on the value of δ, we observe that $c_s - c(a,t)$, and hence $1 - C\left(\tilde{X} = 0, \tilde{T}\right)$, i.e. $1 - C_+\left(\tilde{T}\right)$, will be independent of δ; this is evident since there is no δ in either equation (2.48) or (2.49). Thus, it makes sense to look at $1 - C\left(0, \tilde{T}\right)$ vs. $\tilde{T}$, ahead of considering the solutions for $\tilde{S}$ and $C\left(X, \tilde{T}\right)$. Thus, Fig. 3 shows a log-log plot for $1 - C\left(0, \tilde{T}\right)$ vs. $\tilde{T}$, as well $1 + \mu \tilde{T}^{1/2}$ vs. $\tilde{T}$; the second of these is the small-time approximation
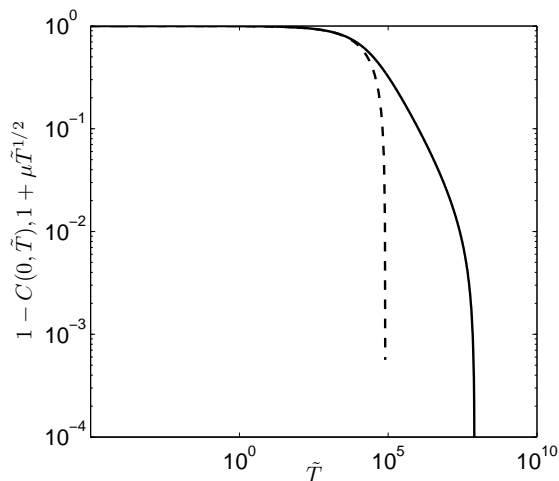
FIG. 3. $1 - C\left(0, \tilde{T}\right)$ (solid line) and $1 + \mu \tilde{T}^{1/2}$ (dashed line) vs. $\tilde{T}$

for $1 - C\left(0, \tilde{T}\right)$ derived in Section 2.3 and makes use of the form for C in (2.70) and (2.80). We see that this approximation works quite well until $\tilde{T} \sim 10^4$, after which the two curves diverge.

In similar vein, Fig. 4 shows $\tilde{S}$ vs. $\tilde{T}$, as well as $\lambda \tilde{T}^{3/4}$ vs. $\tilde{T}$; the latter of these is also from the small-time approximation, as indicated between equations (2.58) and (2.59). Whilst this result does not depend on δ either, we have stopped the computation when $\tilde{S}$ reaches $O\left(10^4\right)$, with a view to exploring the results when $\delta \geqslant 10^{-8}$; this covers the range in δ considered in Vo et al. (2018). Here also, we see that the two curves follow each other until $\tilde{T} \sim 10^4$, at which point $\tilde{S} \sim 10^2$. This would mean that, for $10^{-4} \leqslant \delta \ll 1$, a preliminary estimate for $\tilde{T}$ of when $\tilde{S} = 1/\delta^{1/2}$, which we denote by $\tilde{T}_{stop}$, would be given by

$$\lambda \tilde{T}_{stop}^{3/4} \approx \frac{1}{\delta^{1/2}}, \tag{3.1}$$

giving $\tilde{T}_{stop} \approx \left(\lambda \delta^{1/2}\right)^{-4/3}$. In actual time, this amounts to

$$t_{stop} = a^2 \delta \tilde{T}_{stop} / D_e \left(= a^2 \tilde{T}_{stop} / D_w\right). \tag{3.2}$$

It is also instructive to see the relative errors between the solutions for $1 - C\left(0, \tilde{T}\right)$ and S given in Figs. 3 and 4, respectively; these can be defined as

$$re_C := \left| \frac{1 - C\left(0, \tilde{T}\right) - \left(1 + \mu \tilde{T}^{1/2}\right)}{1 + \mu \tilde{T}^{1/2}} \right| \tag{3.3}$$

and

$$re_S := \left| \frac{\tilde{S} - \lambda \tilde{T}^{3/4}}{\lambda \tilde{T}^{3/4}} \right|, \tag{3.4}$$
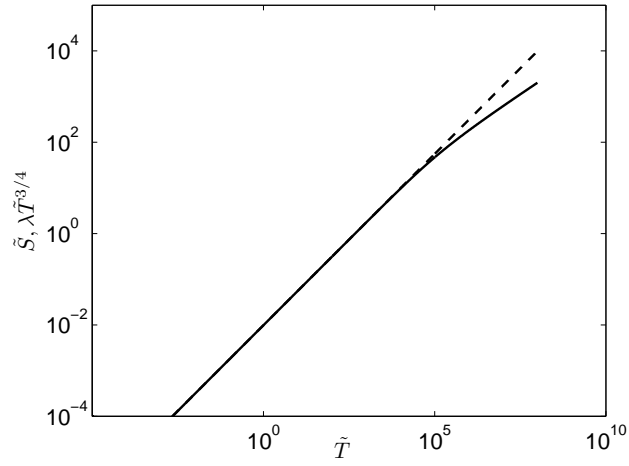
FIG. 4. $\tilde{S}$ (solid line, computed) and $\lambda\tilde{T}^{3/4}$ (dashed line) vs. $\tilde{T}$. Note that the computation has been stopped at $\tilde{T} = 10^8$; at this stage $\tilde{S} \approx 2004$, which implies that $\delta \approx 10^{-7}$. In more detail, with $\tilde{S} = 1/\delta^{1/2}$, we have $\delta = 1/2004^2 = 2.49 \times 10^{-7}$.
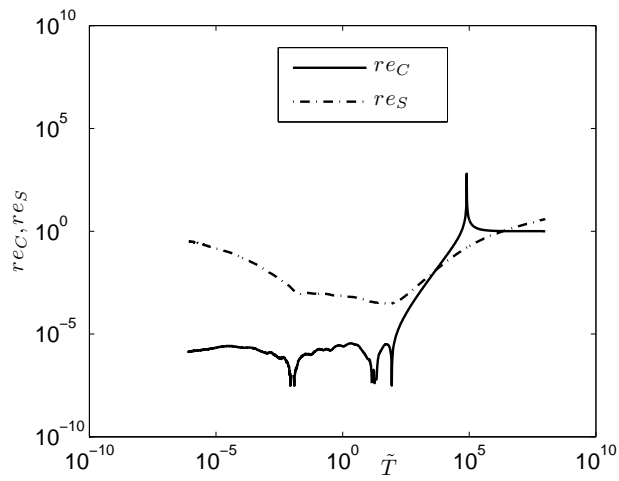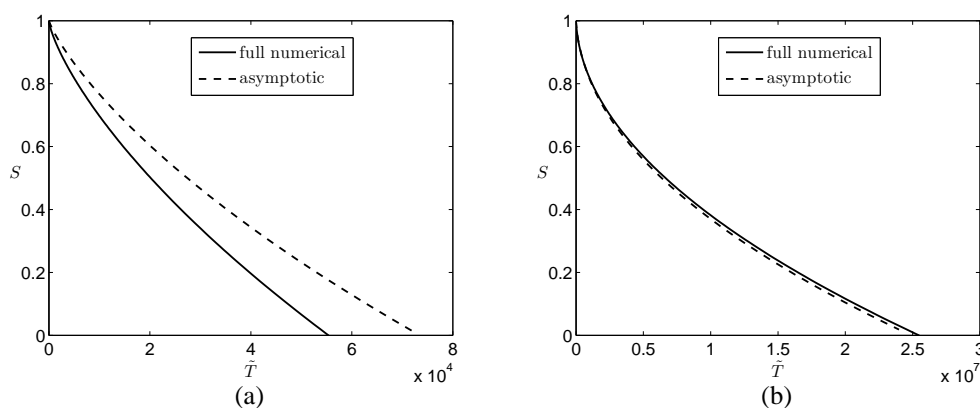

FIG. 5. The relative errors for C and S, re_C and re_S, respectively, vs. $\tilde{T}$.

δ	t_{stop} [days]	
	Fig. 4	Vo et al. (2018)
5×10^{-7}	~ 46.4	~ 46.5
10^{-6}	~ 23.8	~ 23
5×10^{-6}	~ 4.97	~ 5
10^{-5}	~ 2.6	~ 2.5

Table 2. t_{stop}, as calculated in two different ways for four values of δ.

FIG. 6. Comparison of S as a function of $\tilde{T}$, as obtained numerically and via asymptotics, for: (a) $\delta = 10^{-3}$; (b) $\delta = 10^{-6}$

respectively. These are plotted as functions of $\tilde{T}$ in Fig. 5. As might have been expected from Figs. 3 and 4, the relative errors are quite small until $\tilde{T} \sim 10^4$.

However, the values for δ used in Vo et al. (2018) lie outside of the aforementioned range - they are smaller - and any attempt to use equation (3.1) can thus be expected to underestimate the value of t_{stop}. Instead, in Table 2, we compare the values of t_{stop} as given by the solid line in Fig. 4, which were obtained from the solution of (2.54)-(2.57), and as estimated from Fig. 3 in Vo et al. (2018), for different values of δ. As can be seen, the qualitative and quantitative agreement is very good.

A further indication of the correctness of the asymptotic result is a comparison with the numerical solution of the full original equations as δ decreases. This is shown in Fig. 6, where the profiles for S are compared for $\delta = 10^{-3}$ and $\delta = 10^{-6}$. As can be seen, the profiles in Fig. 6(b) for the lower value of δ agree very well, although this cannot be said to be the case for the profiles in Fig. 6(a) for the higher value.

An interesting observation now arises: if D_w, L_d/a and c_0/c_s are fixed, only one computation, i.e. the one that was already carried out already to determine the profile for $\tilde{S}$ and which generated the results for Fig. 4, is required to find the solution for $C\left(X, \tilde{T}\right)$, which comes from the solution for F via equation (2.53), for any value of δ! This is as opposed to having to carry out a new computation on each occasion that D_e, and hence δ, is changed, as was done in Vo et al. (2018). To see this, we show
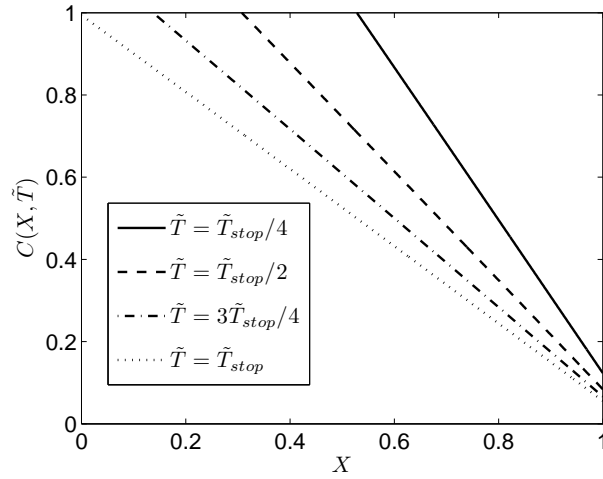
FIG. 7. C vs. X for four different values of $\tilde{T}$ for $\delta = 10^{-5}$, as obtained by solving (2.54), subject to (2.55)-(2.57). $\tilde{T}_{stop}$ corresponds to t_{stop} =2.6 days.
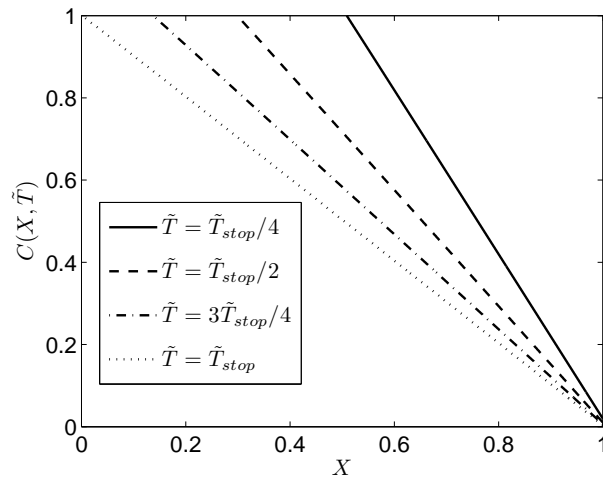

FIG. 8. C vs. X for four different values of $\tilde{T}$ for $\delta = 5 \times 10^{-7}$, as obtained by solving (2.54), subject to (2.55)-(2.57). $\tilde{T}_{stop}$ corresponds to t_{stop} =46.4 days.

in Figs. 7 and 8 C as a function of X for $\tilde{S}\left(\tilde{T}\right) \leqslant X \leqslant 1$ for four different values of $\tilde{T}$ for $\delta = 10^{-5}$ and 5×10^{-7}, respectively; note that, in these figures, the concentration profile at $\tilde{T} = 0$, corresponding to $t = t_a$, consists of a point that is located at $C = 1$ and $X = 1$ but which then become a curve - a line, as it turns out - that moves down and to the left with time. In both figures, X is related to the independent variables of the domain in which the computations were carried out, η and $\tilde{T}$, by

$$X = 1 - \delta^{1/2} \eta \tilde{S}\left(\tilde{T}\right),$$

as can be seen by tracking back through the substitutions in equations (2.8), (2.22) and (2.53).

4. Discussion

This paper has considered the asymptotic analysis of a recent model by Vo et al. (2018) for drug release from polymer-free coronary stents with microporous surfaces; this was originally treated as a one-dimensional, transient, one-phase, diffusion-controlled moving boundary problem occuring over two layers having widely differing diffusivities, with the moving front passing with time from the layer with higher diffusivity to the layer with lower. Although there is a similarity solution whilst the front is in the first layer, this is not the case when the front is in the second. With the ratio of the diffusivities, δ, as an asymptotically small parameter, the analysis indicates how the solutions in the two layers can be decoupled, leading to a numerical formulation that is less demanding to solve computationally; the results are found to agree well with the numerical solution to the full problem as $\delta \to 0$, as would be hoped. Nevertheless, there are at least two notable findings which were either not commented on, or not obvious, in the original work by Vo et al. (2018):

- as that work was carried out in dimensional variables, there was no indication as to how the time taken for the front to reach the stent surface depended on the model parameters - this becomes much clearer with the current approach;

- it now turns out that, regardless of the value of the lower diffusivity in the second layer, it is possible to determine the above-mentioned time to reasonable accuracy with just one computation, rather than having to do multiple computations for different values, as explained in the last paragraph of section 3.

In a wider context, the significance of the work is to suggest how a complex problem having a small diffusivity ratio may be simplified asymptotically, without any loss of the original physics, to give a formulation that is mathematically more transparent and cheaper to compute. In the drug-delivery context, this idea may be useful for prototyping, since it is not known *a priori* what a suitable value of δ should be, other than that it is most likely to be small. Moreover, although the analysis here has been carried out in just one spatial dimension, the principle can be expected to be of use in higher dimensions also.

Acknowledgment

Appendix A: numerical solution of the full equations

We require to solve (2.9)-(2.16). Although a numerical solution for the problem was given by Vo et al. (2018) using a finite-difference method, here we apply an alternative approach that employs recent developments in the solution of Stefan problems for which the domain of interest initially has zero thickness (Mitchell & Vynnycky (2009, 2014, 2016)). For this, we use boundary immobilization for $S(T) < X < 1$ by setting

$$\eta = \frac{X - S(T)}{1 - S(T)}. \tag{A.1}$$

The governing equations are then

$$\delta \frac{\partial C}{\partial T} = \frac{\partial^2 C}{\partial X^2}, \qquad 1 < X < \infty, \quad T > 0, \tag{A.2}$$

$$(1-S)^2 \frac{\partial C}{\partial T} + \dot{S}(1-S)(\eta-1)\frac{\partial C}{\partial \eta} = \frac{\partial^2 C}{\partial \eta^2}, \qquad 0 < \eta < 1, \quad T > 0, \tag{A.3}$$

subject to the boundary conditions

$$C = 1, \quad -\frac{\partial C}{\partial \eta} = (1-S)\frac{dS}{dT}\left(1 - \frac{c_0}{c_s}\right), \quad \text{at } \eta = 0, \tag{A.4}$$

$$C \to 0, \quad \text{as } X \to \infty, \tag{A.5}$$

$$[C]_-^+ = 0 \quad \text{at } X = 1, \tag{A.6}$$

$$\frac{\delta}{1-S}\left(\frac{\partial C}{\partial \eta}\right)_{\eta=1} = \left(\frac{\partial C}{\partial X}\right)_{X=1}. \tag{A.7}$$

and the initial conditions

$$S(0) = 1, \quad C(X,0) = C_a(X), \quad X \geqslant 1. \tag{A.8}$$

In the limit as $T \to 0$ as $S \to 1$, (A.3) gives

$$\frac{d^2 C}{d\eta^2} = 0, \qquad 0 < \eta < 1, \tag{A.9}$$

subject to

$$C = 1, \quad \frac{dC}{d\eta} = 0, \quad \text{at } \eta = 1, \tag{A.10}$$

$$C = C_a(1), \quad \frac{dC}{d\eta} = 0, \quad \text{at } \eta = 0. \tag{A.11}$$

Although this system appears to be overspecified, since there are four boundary conditions for a second-order ordinary differential equation, the fact that $C_a(1) = 1$ means that

$$C \equiv 1 \tag{A.12}$$

satisfies (A.9)-(A.11), and can therefore constitute the initial condition for $0 < \eta < 1$.

This reformulated problem, consisting of (A.2) and (A.3) subject to the boundary conditions (A.4) and (A.7) and initial conditions (A.8) and (A.12), was solved using the finite-element software, Comsol

Multiphysics, which has recently been employed for a number of other Stefan-like problems; see, for example, Vynnycky (2016), Vynnycky & Saleem (2017) and Vynnycky et al. (2018). For the numerical solution, the 1D transient mode of Comsol Multiphysics was used, in tandem with 20000 uniform Lagrangian quadratic elements in space, corresponding to around 40000 degrees of freedom. The convergence criterion at each time step was taken as

$$
\left(\frac{1}{N_{\text{dof}}} \sum_{i=1}^{N_{\text{dof}}} \left(\frac{|E_i|}{A_i + R|U_i|} \right)^2 \right)^{\frac{1}{2}} < 1, \tag{A.13}
$$

where (U_i) is the solution vector corresponding to the solution at each time step, A_i is the absolute tolerance for the ith degree of freedom, R is the relative tolerance and N_{dof} is the number of degrees of freedom; for the computations, $R = 10^{-6}$, $A_i = 10^{-7}$ for $i = 1, .., N_{\text{dof}}$.

We can also note that although the number of elements used may appear to be excessive, it proves to be necessary in order that the numerical scheme accurately accounts for the asymptotic decay of C as $X \to \infty$; in turn, this is linked to the value of X that is used as the outer edge of the computational domain. A guide for what this value should be comes from the form for $C_a(X)$, i.e. equation (2.14): with the parameter values in Table 1, we find that we need $X \sim 10^3$ to ensure that $C_a(X) \sim 10^{-6}$. For this reason, we set the outer edge of the computational domain at $X = 10^3$; thus, the size of each element in the spatial variable was 0.05.

Lastly, we point out that these considerations are not required for the numerical solution of the asymptotically reduced equations, since there is no need to solve numerically for $X > 1$; as a consequence, far fewer mesh elements are required and, moreover, these only need to be deployed in the region where $X < 1$. For reference, we note that, for those computations, 480 elements were used, corresponding to $N_{\text{dof}} = 960$; the same values of R and A_i were used as indicated in the previous paragraph.

REFERENCES

Anderson, C. A. (1982) A new picture of the raw-wool fiber. *J. Text. Inst.*, **73**, 289–292.

Bakal, A., Timbers, G. & Hayakawa, K. (1970) Solution of the characteristic equation involved in the transient heat conduction for foods approximated by an infinite slab. *Can. Inst. Food Technol. J.*, **3**, 76–77.

Briozzo, A. C., Natale, M. F. & Tarzia, D. A. (2007) Existence of an exact solution for a one-phase Stefan problem with nonlinear thermal coefficients from Tirskii's method. *Nonlin. Anal. - Theory Meth. Applics.*, **67**, 1989–1998.

Carslaw, H. S. & Jaeger, J. C. (1959) *Conduction of Heat in Solids*. Oxford University Press, USA, 2$^{\text{nd}}$ edition.

Cho, S. H. & Sunderland, J. E. (1974) Phase-change problems with temperature-dependent thermal-conductivity. *J. Heat Transfer*, **96**, 214–217.

Cohen, D. S. & Erneux, T. (1988a) Free-boundary problems in controlled release pharmaceuticals. 1. Diffusion in glassy-polymers. *SIAM J. Appl. Math.*, **48**, 1451–1465.

Cohen, D. S. & Erneux, T. (1988b) Free-boundary problems in controlled release pharmaceuticals. 2. Swelling-controlled release. *SIAM J. Appl. Math.*, **48**, 1466–1474.

Conti, M. (2001) Density change effects on crystal growth from the melt. *Phys. Rev. E*, **64**, Article no. 051601.

Crank, J. (1984) *Free and moving boundary problems*. Clarendon Press, Oxford.

El-Hasadi, Y. M. F. & Khodadadi, J. M. (2013) One-dimensional Stefan problem formulation for solidification of nanostructure-enhanced phase change materials (NePCM). *Int. J. Heat Mass Transfer*, **67**, 202–213.

Fan, L. W., Zhu, Z. Q. & Liu, M. J. (2015) A similarity solution to unidirectional solidification of nano-enhanced phase change materials (NePCM) considering the mushy region effect. *Int. J. Heat Mass Transfer*, **86**, 478–481.

Fila, M. & Souplet, P. (2001) Existence of global solutions with slow decay and unbounded free boundary for a superlinear Stefan problem. *Interfaces Free Boundaries*, **3**, 337–344.

Furzeland, R. (1980) A comparative study of numerical methods for moving boundary value problems. *IMA J. Appl. Maths*, **26**, 411–429.

Gotz, I. G. & Zaltzman, B. (1995) Two-phase Stefan problem with supercooling. *SIAM J. Math. Anal.*, **26**, 694–714.

Gupta, S. C. (2003) *The Classical Stefan Problem: basic concepts, modeling and analysis,*. Elsevier, Amsterdam.

Hill, J. M. & Hart, V. G. (1986) The Stefan problem in nonlinear heat conduction. *Z. Angew. Math. Phys*, **37**, 206–229.

Hill, J. M. (1987) *One-dimensional Stefan Problem: an introduction*. Longman Scientific and Technical, New York.

King, J. R. & Evans, J. D. (2005) Regularization by kinetic undercooling of blow-up in the ill-posed Stefan problem. *SIAM J. Appl. Maths*, **65**, 1677–1707.

Libbrecht, K. G. (2005) The physics of snow crystals. *Rep. Prog. Phys.*, **68**, 855–895.

Lorenzo-Trueba, J. & Voller, V. R. (2010) Analytical and numerical solution of a generalized Stefan problem exhibiting two moving boundaries with application to ocean delta formation. *J. Math. Anal. Appl.*, **366**, 538–549.

McCue, S. W., Wu, B. & Hill, J. M. (2008) Classical two-phase Stefan problem for spheres. *Proc. Roy. Soc. A*, **464**, 2055–2076.

McCue, S. W., Wu, B. & Hill, J. M. (2009) Micro/nanoparticle melting with spherical symmetry and surface tension. *IMA J. Appl. Maths*, **74**, 439–457.

McGinty, S., Vo, T. T. N., Meere, M., McKee, S. & McCormick, C. (2015) Some design considerations for polymer-free drug-eluting stents: A mathematical approach. *Acta Biomaterialia*, **18**, 213–225.

Mehling, H. & Cabeza, L. F. (2002) *Heat and Cold Storage with PCM*. Springer, Berlin.

Mitchell, S. L. & Vynnycky, M. (2009) Finite-difference methods with increased accuracy and correct initialization for one-dimensional Stefan problems. *Appl. Math. Comp.*, **215**, 1609–1621.

Mitchell, S. L. & Vynnycky, M. (2014) On the numerical solution of two-phase Stefan problems with heat-flux boundary conditions. *J. Comp. Appl. Maths*, **264**, 49–64.

Mitchell, S. L. & Vynnycky, M. (2016) On the accurate numerical solution of a two-phase Stefan problem with phase formation and depletion. *J. Comp. Appl. Maths*, **300**, 259–274.

Natale, M. F. & Tarzia, D. (2003) Explicit solutions to the one-phase Stefan problem with temperature-dependent thermal conductivity and a convective term. *Int. J. Eng. Sci.*, **41**, 1685–1698.

Ockendon, J. R. (1975) Techniques of analysis. In *Heat Balance Methods in Melting Problems: moving boundary problems in heat flow and diffusion (Editors: Ockendon, J. R. & Hodgkins, W. R.), University of Oxford, UK, 25-27 March 1974*, pages 138–149.

Ockendon, J. R. & Hodgkins, W. R. (1975) *Heat Balance Methods in Melting Problems: moving boundary problems in heat flow and diffusion*. Clarendon Press, Oxford.

Paul, D. R. & McSpadden, S. K. (1976) Diffusional release of a solute from a polymer matrix. *J. Membrane Sci.*, **1**, 33–48.

Rogers, C. (1986) On a class of moving boundary problems in non-linear heat conduction: application of a Bäcklund transformation. *Int. J. Nonlin. Mech.*, **21**, 249–256.

Schmidt, A. (1996) Computation of three dimensional dendrites with finite elements. *J. Comput. Phys.*, **125**, 293–312.

Segal, G., Vuik, K. & Vermolen, F. (1998) A conserving discretization for the free boundary in a two-dimensional Stefan problem. *J. Comput. Phys.*, **141**, 1–21.

Sharifi, N., Bergman, T. L., Allen, M. J. & Faghri, A. (2014) Melting and solidification enhancement using a combined heat pipe, foil approach. *Int. J. Heat Mass Transfer*, **78**, 930–941.

Shen, Z. H., Zhang, S. Y., Lu, J. & Ni, X. W. (2001) Mathematical modeling of laser induced heating and melting in solids. *Optic. Laser Technol.*, **33**, 533–537.

Stefan, J. (1890) Über die Theorie der Eisbildung. *Monatshefte für Mathematik und Physik*, **1**, 1–6.

Struckmeier, J. & Unterreiter, A. (2001) A singular-perturbed two-phase Stefan problem. *Appl. Math. Lett.*, **14**, 217–222.

Tabakova, S., Feuillebois, F. & Radev, S. (2010) Freezing of a supercooled spherical droplet with mixed boundary conditions. *Proc. Roy. Soc. A*, **466**, 1117–1134.

Tarzia, D. A. (2011) Explicit and Approximated Solutions for Heat and Mass Transfer Problems with a Moving Interface. In *Advanced Topics in Mass Transfer (Editor: El-Amin, M.), IntechOpen, Rijeka*, ch. 20.

Tayler, A. B. (1975) The mathematical formulation of Stefan problems. In *Heat Balance Methods in Melting Problems: moving boundary problems in heat flow and diffusion (Editors: Ockendon, J. R. & Hodgkins, W. R.), University of Oxford, UK, 25-27 March 1974*, pages 120–137.

Trelles, J. P. & Dufly, J. J. (2003) Numerical simulation of porous latent heat thermal energy storage for thermoelectric cooling. *Appl. Therm. Eng*, **23**, 1647–1664.

Vo, T. T. N., Morgan, S., McCormick, C., McGinty, S., McKee, S. & Meere, M. (2018) Modelling drug release from polymer-free coronary stents with microporous surfaces. *Int. J. Pharm.*, **544**, 392–401.

Voller, V. (2006) A similarity solution for solidification of an under-cooled binary alloy. *Int. J. Heat Mass Transfer*, **49**, 1981–1985.

Voller, V. R. & Falcini, F. (2013) Two exact solutions of a Stefan problem with varying diffusivity. *Int. J. Heat Mass Transfer*, **58**, 80–85.

Vuik, C. & Cuvelier, C. (1985) Numerical solution of an etching problem. *J. Comput. Phys.*, **59**, 247–263.

Vynnycky, M. (2016) An asymptotic model for the primary drying stage of vial lyophilization. *J. Engng Maths*, **96**, 175–200.

Vynnycky, M. & Saleem, S. (2017) On the explicit resolution of the mushy zone in the modelling of the continuous casting of alloys. *Appl. Math. Mod.*, **50**, 544–568.

Vynnycky, M., Saleem, S. & Fredriksson, H. (2018) An asymptotic approach to solidification shrinkage-induced macrosegregation in the continuous casting of binary alloys. *Appl. Math. Mod.*, **54**, 605–626.

Zalba, B., Marin, J. M., Cabeza, L. F. & Mehling, H. (2003) Review on thermal energy storage with phase change: materials, heat transfer analysis and applications. *Appl. Therm. Eng.*, **23**(3), 251–283.